Powder Technology 428 (2023) 118842

Contents lists available at ScienceDirect

Powder Technology

journal homepage: www.journals.elsevier.com/powder-technology

Effect of bevelled silo outlet in the flow rate during discharge

Paula A. Gago [a,*], Marcos A. Madrid [b,c], Stefan Boettcher [d], Raphael Blumenfeld [a], Peter King [a]

[a] Department of Earth Science and Engineering, Imperial College, London, SW7 2BP, UK
[b] Departamento de Ingeniería Mecánica, Facultad Regional La Plata, Universidad Tecnológica Nacional, CONICET, Avenida 60 Esquina 124, 1900 La Plata, Buenos Aires, Argentina
[c] Instituto de Física de Líquidos y Sistemas Biológicos, CONICET, 59, 789, 1900 La Plata, Argentina
[d] Department of Physics, Emory University, Atlanta, USA

HIGHLIGHTS

- Bevelled silo outlets increase the flow rate.
- Quasi-two-dimensional silo, DEM.
- Realistic operation conditions.

GRAPHICAL ABSTRACT

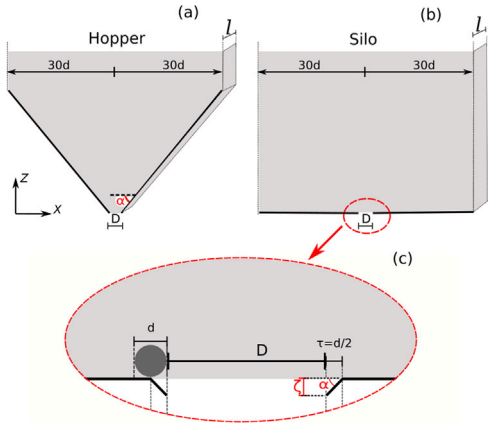

ARTICLE INFO

Keywords:
DEM
Silo discharge
Bevelled silo outlet

ABSTRACT

We investigate the effect of a bevelled (or slanted) outlet on the discharge rate of mono-sized spheres from a quasi-two-dimensional silo, using the discrete element method. In contrast to hopper discharges, where the bevelling is across the entire base of the container, we study a bevelled opening that is significantly smaller than the silo width and in which the slanting is limited to half a sphere diameter at the boundary of the outlet. We show that the bevelling increases the flow rate comparably to the inclination in hopper walls. Using Beverloo's model, we relate this increase in rate to what we define as the 'effective opening' of the silo and analyse the velocity profiles associated with the discharges. We show that different openings, having effectively the same discharge rates, give rise to distinctly different internal dynamics in the silo. These results have the potential to aid industrial processes by fine-tuning and improving control of silo discharges, with a minimal impact on silo design, thus significantly reducing production and handling costs.

1. Introduction

The flow of granular materials through narrow exits, which occurs regularly in everyday life, is a rich and complex process. Being of particular technological interest, silo discharges have been widely studied [1–12]. Gravity-driven discharges of granular material are known to be at constant rate, which is the reason that hour glasses are filled with particulates rather than liquids. It has been shown that the rate of volume discharge, W, is a function of the ratio of the silo aperture diameter, D, to the typical grain size (diameter), d [13,14]. Beverloo [13] proposed an empirical relation between W and the system properties

* Corresponding author.
E-mail address: paulaalejandrayo@gmail.com (P.A. Gago).

https://doi.org/10.1016/j.powtec.2023.118842
Received 27 February 2023; Received in revised form 24 May 2023; Accepted 26 July 2023
Available online 29 July 2023

that, for quasi-two-dimensional silos, can be written as [15]

$$W = C\phi_b g^{1/2}(D - kd)^{3/2} l \ , \tag{1}$$

where k and C are two dimensionless fitting constants, ϕ_b is the bulk packing fraction of the granular medium, l is the thickness of the gap between the parallel plates (defining the quasi-two-dimensional cell), and g the gravitational acceleration. Beverloo's rule is normally explained by heuristic models such as the 'Free-Fall Arch' [16] and the 'Empty Annulus' [17]. The Free-Fall Arch model is based on the idea that most grains lose contact with the rest of the granular packing when they are about one orifice radius, $D/2$, above the outlet and that particles at this point fall freely from an initial zero vertical velocity. Free-falling over this height leads to a flow rate proportional to $g^{1/2}D^{3/2}l$ in quasi $2D$ systems, irrespective of material properties and column height in the silo. The Empty Annulus model [18] is based on the idea that the effective outlet opening diameter is $(D - kd)$ because spherical grains cannot pass through an annular zone of width $(1/2)kd$. It has been demonstrated later that, in fact, no such empty annulus exists and the particles near the edge of the orifice are retarded by some dynamics that are not yet fully understood [17]. The value of k has been found to vary by up to a factor of 2, depending on the grains used, but C appears to remain constant practically for any material tested [17]. Nevertheless, some deviations have been observed for very low-friction materials [19] and for different grain shapes [20–22]. Recently, it was shown that this rule can be obtained with the Navier–Stokes equations, applied to plastic fluids and using a constitutive relation for the effective friction based on the $\mu(I)$-rheology [23]. In the following, we will consider a constant material bulk packing fraction, and define a proportionality constant $\tilde{C} \equiv C\phi_b l$.

To study the effects of various parameters, experimental designs in the literature often use an outlet with sharp corners. A departure from sharp corners of 3D hoppers has been studied in [24], but they only considered the convex-lips shape observed as a result of abrasion and wear following discharge. They have shown, numerically and experimentally, that such a curved outlet increases the discharge rate. Here, we focus on the effects of shaped outlet geometries on the silo discharge rate, both because perfectly sharp corners are only an idealisation and because designing the outlet shape can improve discharge rate. Using numerical simulations, we investigate in detail the impact of the outlet bevel parameters on the discharge rate in model quasi-2D silos, focusing on outlet shapes that are not much larger than several grains. To the best of our knowledge, the effects in this range of sizes, which are much smaller than those studied in previous works [2,14,25], have not been investigated systematically. The investigation of this regime is also directly relevant to flow of particulates through sieves of weaved wires.

This paper is structured as follows. The numerical method and the setup are described in Section 2. In Section 3, we present the results obtained when varying the parameters of the bevelled outlets and compare them with known discharge rates in hoppers. In this section, we also extend the Beverloo model and define an effective opening that depends on the slant angle. We conclude in Section 4 with a discussion of the implications that our results have for several applications and suggestions for future work.

2. Methods

We use the discrete element method (DEM) implementation of soft sphere dynamics of *LIGGGTHS* [26]. The material parameters are: inter-particle friction coefficient $\mu = 0.5$, Young's modulus $Y = 10^8$N m^{-2}, Poisson's ratio $\nu = 0.5$, and restitution coefficient $\epsilon = 0.5$. The system is quasi-2D, comprising two parallel plates, a distance $l = 1.1d$ apart, between which lies an assembly of same-size spheres of diameter $d = 1$ mm. Defining gravity as directed vertically, the horizontal system size is $60d$, representing a silo with an outlet at the centre of the base, $30d$ from the 'wall', although periodic boundary conditions are imposed in the horizontal direction to circumvent finite size effects. Five outlet sizes have been investigated: $D = (5, 5.5, 6, 6.5, 7)d$. This range of openings was chosen because there is a higher probability of jamming at the outlet for smaller ones [27].

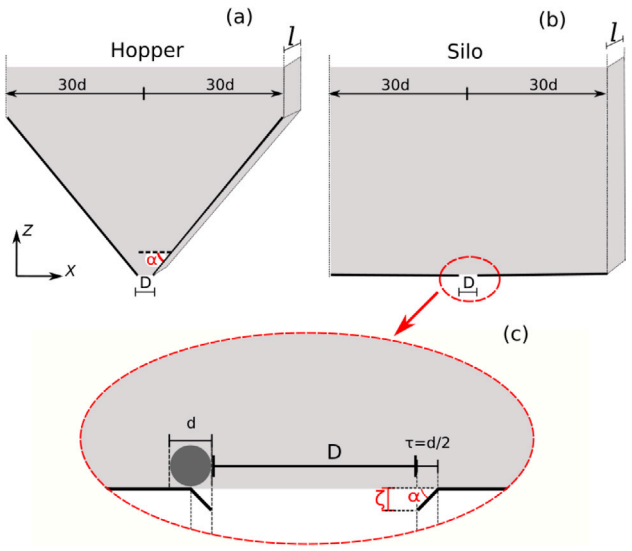

Fig. 1. Sketch of the setup. (a) A quasi-bidimensional hopper, with walls inclined at angle α; (b) a quasi-bidimensional silo with flat bottom and bevelled outlet at angle α; In both cases, the separation between the parallel plates (defining the quasi-two-dimensional cell) is $l = 1.1d$, with d the diameter of the (mono-dispersed) grains. (c) The outlet structure, detailing the constant horizontal projection $\tau = d/2$ and the variable $\zeta = \tau \tan\alpha$.

We have used two designs: a silo with an outlet bevelled at angle α and, for comparison, a hopper with walls inclined at the same angles. In Fig. 1(a) we show a sketch of a hopper, whose inclination, α, is defined as the angle between the horizontal and the wall. In Fig. 1(b) we show a sketch of a silo with a bevelled outlet at an angle α. In Fig. 1(c), the definition of the bevel angle is detailed. The horizontal projection of the slant is kept constant, $\tau = 0.5d$, and the outlet depth was varied $\zeta = \tau \tan\alpha$.

The initial state of each realisation was obtained by pouring 6000 spheres of diameter $d = 1$ mm and density $\rho = 2500$kg m^{-3} into the container, with the outlet closed. The spheres were allowed to settle into mechanical equilibrium, which was determined as the state of total kinetic energy $k_e < 0.001$J. The outlet was then opened abruptly and the number of grains remaining in the silo was measured as a function of time, while the silo emptied. The discharge was considered completed when less than 1000 grains remained. For smaller apertures jamming was observed during the discharge. Numerically, jamming was determined by comparing the number of grains in the silo at intervals of 0.05s. If the number of grains between one of these intervals remained unchanged, and the kinetic energy of the system fell below $k_e < 0.001$J, the system was considered jammed. Simulations ended in jamming were discarded.

We investigated 75 silo systems and 45 hopper systems, each with different parameters. We ran 91 realisations for each angle for cases $D = 5, 5.5$ and $6d$. Of these $\sim 25\%$ of the runs were discarded because of jamming. We ran 21 realisations for the remaining apertures ($D = 6.5$ and $7d$, only for the bevelled silo). These cases did not presented jamming. In total, 8820 discharges were simulated.

Fig. 2 shows, on the left, a screenshot of the initial configuration for the silo (in this screenshot, the outlet shows a bevel angle of 70°). The four panels on the right show a close up of the beginning of the discharge for bevel angles of 0°, 30°, 45°, and 70°. Colour scale in the grains highlights their speed. Here it is possible to see that, although the value of the parameter ζ (Fig. 1(c)) increases as the angle α increases, its value is still of the order of a few grain diameters (for example, $\zeta \approx 1.4d$ for $\alpha = 70°$).

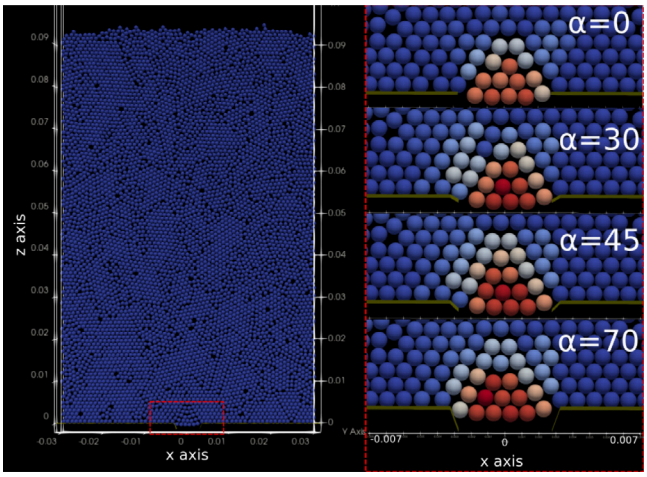

Fig. 2. Left - Initial configuration of 6000 grains in a bevel silo (with a bevel angle of 70°). Right - close-up of the silo outlet (as marked in the red dashed-line rectangle on the left) for four characteristic bevel inclinations: 0°, 30°, 45°, and 70°. Colour scale in the grains highlights their speed.

3. Results

In Fig. 3(a) we show the total discharged volume of spheres from a bevelled silo of opening $D = 5.5d$ as a function of time for several angles α. For clarity, only $\alpha = 0°$, 30°, 45°, and 70°are highlighted. In Fig. 3(b) we show the same results for a hopper with the same values of α.

In Fig. 4(a) we show the volume discharge rate, W, as a function of α for the different apertures of the bevelled outlet silo (open symbols/dashed lines). In the same figure and with filled symbols, we show the equivalent behaviour for different hopper inclinations (only for apertures $5d$, $5.6d$, $6d$). In this figure it is possible to see that the rate of discharge of both systems increases with the inclination α.

Results for the hopper increasing their discharge rate with α are consistent with those presented in the literature [14,25], although we do not capture the non-monotonic flow rate behaviour reported for small hopper angles. Although the change of the mass rate with α is almost identical for both systems for smaller angles, for bigger $\alpha(> 50°)$ the hopper increase in discharge rate results bigger than that of a silo with identical bevel inclination. The deviation between silo and hopper becomes more evident in Fig. 4(b), that shows the same than (a) but with the rates $W(\alpha)$ normalised by the rate corresponding to the discharge with zero angle $W(\alpha = 0)$.

From Fig. 4(b) we can also appreciate that the increase of the rate (with respect to $\alpha = 0$) is higher in both cases, bevelled silo and hopper, for smaller apertures than for bigger ones (see for example the orange circle, $D = 5d$, and the magenta triangle, $D = 6d$, at $\alpha = 70°$).

In Fig. 5(a) we show W as a function of D for a selection of angles α, for clarity. The data were fitted to Eq. (1) to obtain the parameters k and $\tilde{C}$. We find that the value of $\tilde{C}$ is nearly constant for all the curves and, therefore, we averaged them and obtained $\tilde{C} = 1.32(1)$ cm. We then used this value to obtain a fit for the value of k.

As mentioned, a widely accepted interpretation of the parameter k in Eq. (1) is that it accounts for an empty annulus [18], i.e., a region around the orifice in which particles are constrained from moving, effectively restricting the opening to $D - k\,d$. Rewriting the values $k(\alpha)$, obtained from our fitting of Eq. (1), as

$$k(\alpha) = k_0 + \delta k(\alpha)\ , \tag{2}$$

we plot in Fig. 5(b) $\delta k(\alpha)$ as a function of α. We find that δk increases monotonically with α and that it is $d/2$ at $\alpha \approx 45°$ (black dashed circle). At $\alpha = 90°$, we added a square to highlight the expected asymptotic

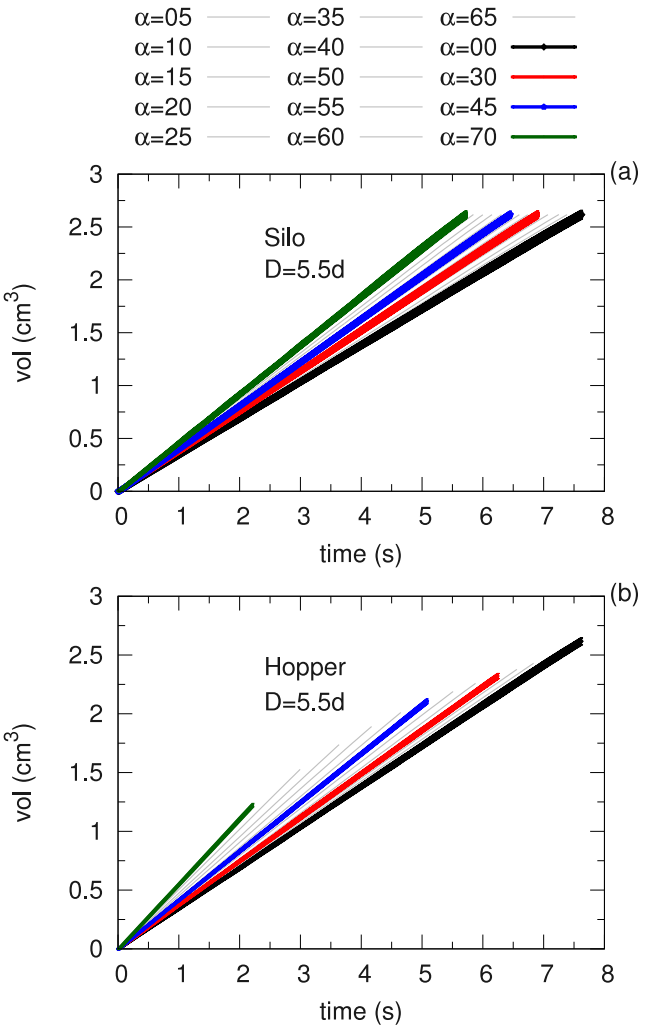

Fig. 3. Discharged volume as a function of the time for: (a) a bevelled silo; (b) a hopper, both with outlet opening of $D = 5.5d$ and several values of α. For clarity, only $\alpha = 0°$, 30°, 45°and 70°are highlighted and display error bars. Error bars were obtained as the standard deviation of the mean over the independent realisations.

behaviour, where the effect of the slant should disappear and the outlet is effectively $2\tau = 1d$ wider than the actual one. The precise form of this curve is not yet understood and modelling it theoretically, which is outside the scope of this work, will be addressed in a future report.

Next, we turn attention to the velocity profiles of the discharge process. We recorded particle velocities during the discharge for 500 frames, with each frame corresponding to 10^{-2}s. The initial 0.1s (10 frames) were discarded to eliminate transient effects. We used this protocol on 10 independent non-jammed realisations. Velocity profiles were measured across an horizontal slice of $2d$ thickness from the bottom of the container.

Fig. 6(a) shows the mean absolute value of the vertical component of the velocity, v_z for silos having different opening apertures Ap (and bevel angle $\alpha = 0$). In this figure, the dashed lines indicate the position of the opening edge ($x = D/2$) for each system (by their corresponding colour). Fig. 6(b) shows the same than (a) but for the horizontal component of the velocity v_x. The displacement observed between these curves is a well known result [2]. It has been also shown that, with a proper rescaling, all profiles can be collapsed.

Fig. 6(c) and (d) show the velocity profiles corresponding to silos with aperture $Ap = 5.5d$ and different bevel angles. The black-dashed line here marks the position of the edge ($x = D/2$) of the outlet, while the grey-dashed one marks the "inflection" point of the bevel

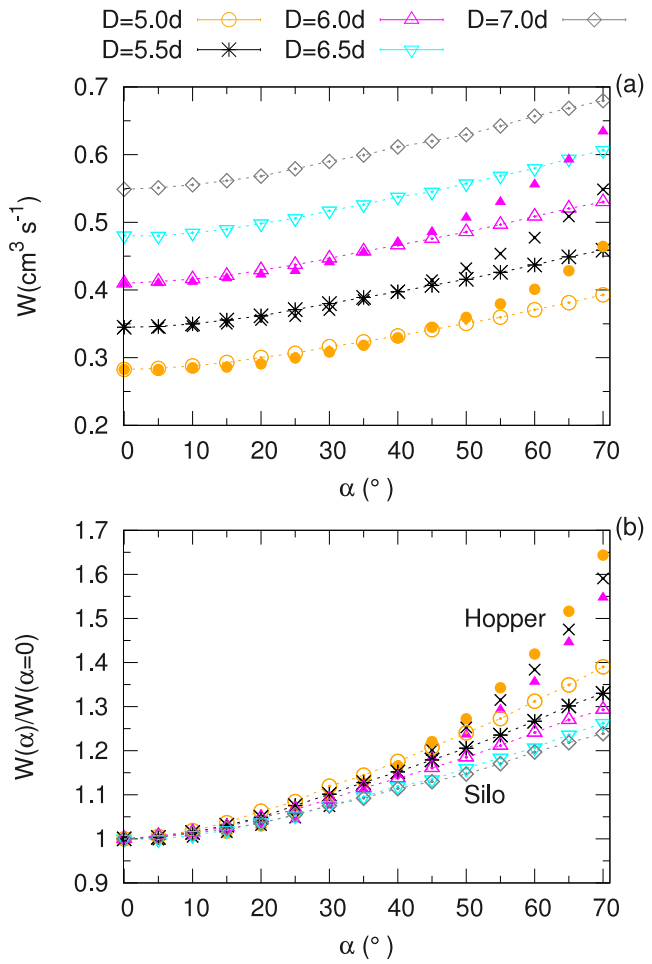

Fig. 4. (a) Volume rate as a function of α for the bevelled silo (open symbols/dashed lines) and the hopper (closed symbols). (b) Same than (a), but with the volume rate as a function of the inclination $W(\alpha)$ normalised for the rate corresponding to a zero inclination $W(\alpha = 0)$.

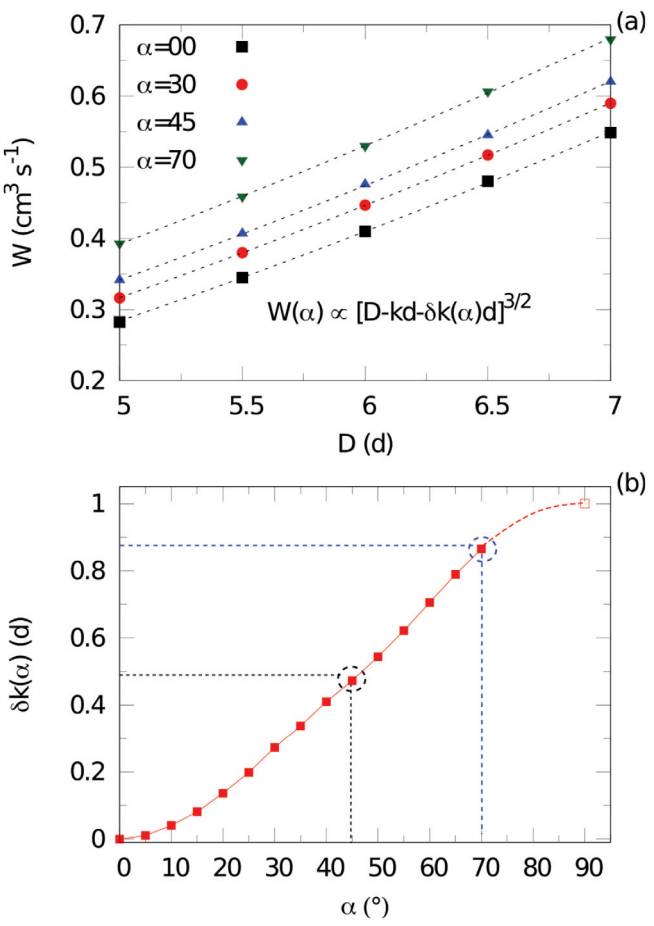

Fig. 5. (a) The discharge rate, W, as a function of the outlet size, D, for a selection of angles; (b) the value of $\delta k(\alpha)$ in Eq. (2), obtained by fitting the data in (a) with the Beverloo model, Eq. (1). The dashed circle highlights the equivalence between an angle $\alpha = 45°$and an effective opening $D_{eff} = D+0.5d$ (black) and an angle $\alpha = 70°$and an effective opening $D_{eff} = D + 0.9d$ (blue). The empty square at $\alpha = 90°$has been added to highlight the expected asymptotic behaviour.

$(x = D/2 + \tau)$. From this figure we can see that, although the flow rate monotonically increases with α, v_z at $x = 0$ does not do the same. On the other hand, v_z at $x = D/2$ does behave monotonically with α.

Fig. 7(a) and (b) show this behaviours at $x = 0$ and $x = D/2$ in more detail for the rest of the apertures studied. In (a), it is possible to see that v_z at $x = 0$ reaches a minimum at $\alpha \sim 30$. Fig. 7(b) highlights the monotonic increase of v_z as a function of α for $x = D/2$.

The horizontal component of the velocity, v_x, in Fig. 6(c) does not exhibit a clear dependence with α near $x = 0$, and it seems monotonically increasing with the bevel angle for $x = D/2$ shown in Fig. 6(d). More statistics would be necessary to have a better characterisation of this variable, in particular, to have a better understanding of the behaviour of the maximum $v_x(\alpha)$.

To finish this analysis, we compare profiles of systems with the same effective opening sizes (as given by they rate of discharge) but different real opening sizes. As we show clearly in Fig. 5 (black dashed circle), a bevel inclination of 45°gives rise to the same flow rate as an opening that is $d/2$ wider. [The inset in Fig. 8(b) demonstrates this equivalence further for the cases $D = 5.5d$ at $\alpha = 45°$(red triangles) and $D = 6d$ at $\alpha = 0°$(blue circles).]

In Fig. 8(a) we show v_z as a function of the distance from the center of the container x. Two different openings with slant angle $\alpha = 0°$are represented in dashed lines, $D_1 = 5.5d$ (open black circles) and $D_2 = 6.0d$ (filled blue circles). Data for an opening of $D_1 = 5.5d$ and $\alpha = 45°$are also shown in red triangles and solid line. Vertical dashed lines mark the positions corresponding to the two outlet openings $x = D_1/2 = 3d$ and $x = D_2/2 = 3.25d$, and the inflection point of the bevel for D_1, $x = D_1/2 + \tau$, see Fig. 1(c). A careful inspection of the velocity profiles of the presumably-equivalent openings $((6d, 45°)$ and $(6.5d, 0°))$ shows that, while they are almost identical for x beyond the effective opening, $x > D_1/2$, they clearly differ for $x < D_1/2$. The maximum difference can be observed at $x = 0$: In this region, the velocity profile seems governed by the real opening size. This difference remains for velocity profiles measured slightly above the container bottom, as shown in Fig. 8(b) (region $L2$, corresponding to $z = (2d - 4d)$), but washes out at layers above $z > 4d$. Above this distance, systems with same equivalent opening exhibit the same vertical velocity profiles.

The horizontal component v_x is shown in Fig. 8(c) and (d) (for $L1$ $(z = (0 - 2d))$ and $L2$ $(z = (2d - 4d))$, respectively). The differences between profiles corresponding to same effective openings is very small for v_x and, as discussed before, more statistics would be necessary to better understand the behaviour of this variable.

4. Discussion

To conclude, we have studied the effects of a bevelled silo outlet on the discharge rate of spheres and on aspects of the internal dynamics.

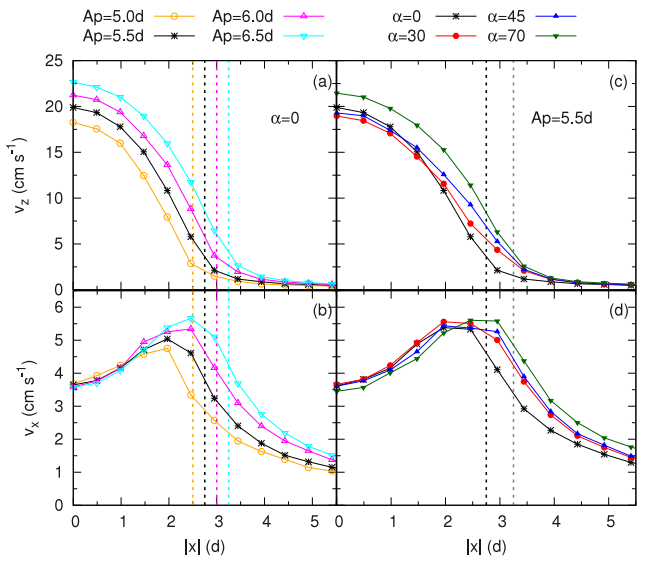

Fig. 6. (a) Absolute mean value for the vertical velocity, v_z, at the bottom of the silo (averaged over grains in the region $z = (0 - 2d)$) for different apertures sizes Ap, as a function of the distance x from the center of the silo. (b) The same than (a) but for the horizontal component of the velocity, v_x. The vertical dashed lines in (a) and (b) indicate the position of the opening edge ($x = D/2$) for each system (by their corresponding colour). (c) Absolute mean value for the vertical velocity, v_z, at the bottom of the silo as a function of the distance x from the center of the silo for a single aperture $Ap = 5.5d$ and different bevel angles. (d) The same than (c) but for the horizontal component of the velocity, v_x. The vertical black-dashed line here marks the position of the edge ($x = D/2$) of the outlet, while the grey-dashed one marks the "inflection" point of the bevel ($x = D/2 + \tau$).

We have shown that bevelling the outlet with a boundary that is as small as one particle radius, leads to a discharge rate that is almost as high as a hopper with the same inclination angle as the bevel. The increase is monotonic in the inclination angle. Nevertheless, we note that, although our results for the hopper are consistent with those presented in the literature, we do not capture the non-monotonic flow rate behaviour reported for small hopper angles [14]. Whether this difference is because of the quasi-2D nature of our setup or our use of mono-disperse spheres remains to be explored.

We have presented a way of defining an effective silo opening, based on the rate of discharge and the Beverloo model, (Eq. (1)). This definition allowed us not only to compare systematically, but also to find equivalence between, openings of different bevel angles and different basic sizes. This allowed us to show that systems exhibiting the same discharge rate are not necessarily equivalent because they can have different flow dynamics near the outlet, which depend on the effective opening and the bevel angle.

There is a crossover effect in the velocity profiles at the bottom of the silo: at $x = 0$ the maximum velocity appears to be governed by the real size of the opening, while at the edge, it appears to be governed mainly by the effective size of the orifice. This could be the basis for the equivalence of the discharge rate between openings with the same effective apertures.

These results are encouraging, as they demonstrate that fine-tuning the discharge rate is possible by controlling the bevel angle of the outlet, in addition to its size. This fine-tuning has a potential for better control in industrial applications, such as pharmaceuticals and transport of particulates in general, with a minimal impact on overall design, thus significantly reducing production and handling costs. Our results also provide a systematic method of comparison and equivalence between bevelled silos and hoppers, which is useful when one or

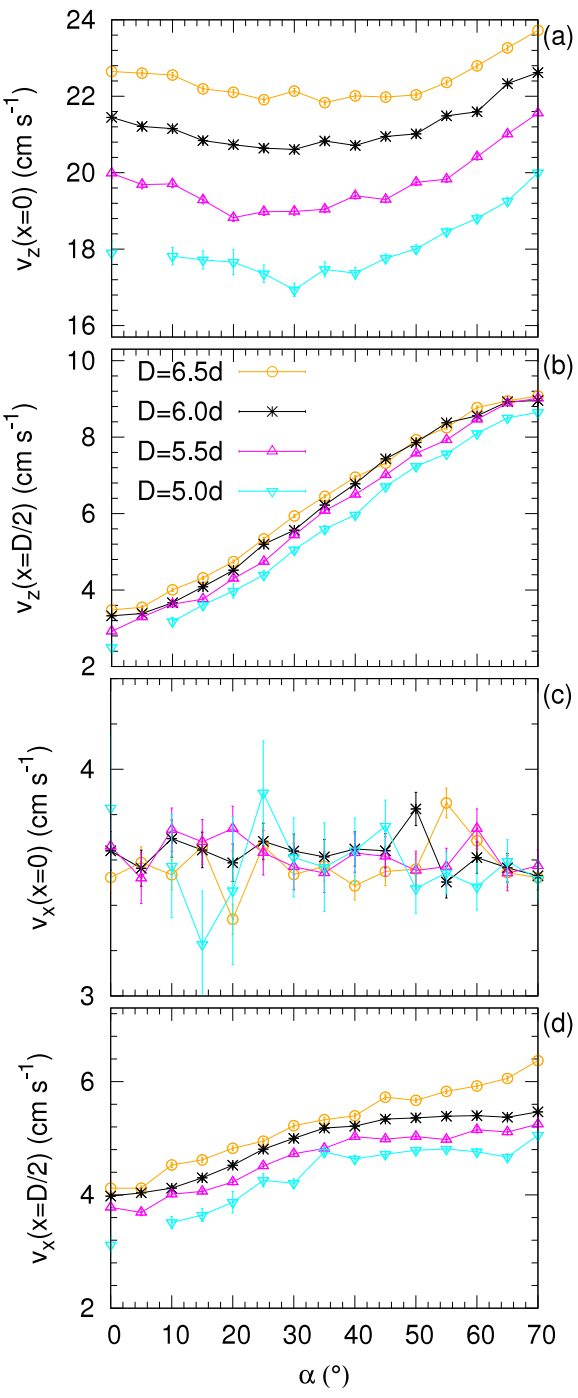

Fig. 7. The dependence of v_z on α at (a) $x = 0$ and (b) $x = D/2$, for opening sizes D between $5d$ and $6.5d$. (c) and (d) The same as in (a) and (b) for v_x.

the other are required for optimal design. These findings also open the door to a better understanding of the effect of wire weaving in sieve design.

There are several physical phenomena at play in the discharge process: the jamming probability at the outlet and the effect of the outlet shape on it, as well as the stress distribution and arching dynamics in the neighbourhood of the outlet. Our results can be used as a benchmark for future work into the theoretical modelling of these phenomena. Further directions to explore would be varying the sphere size distribution, shapes, friction coefficient, etc.

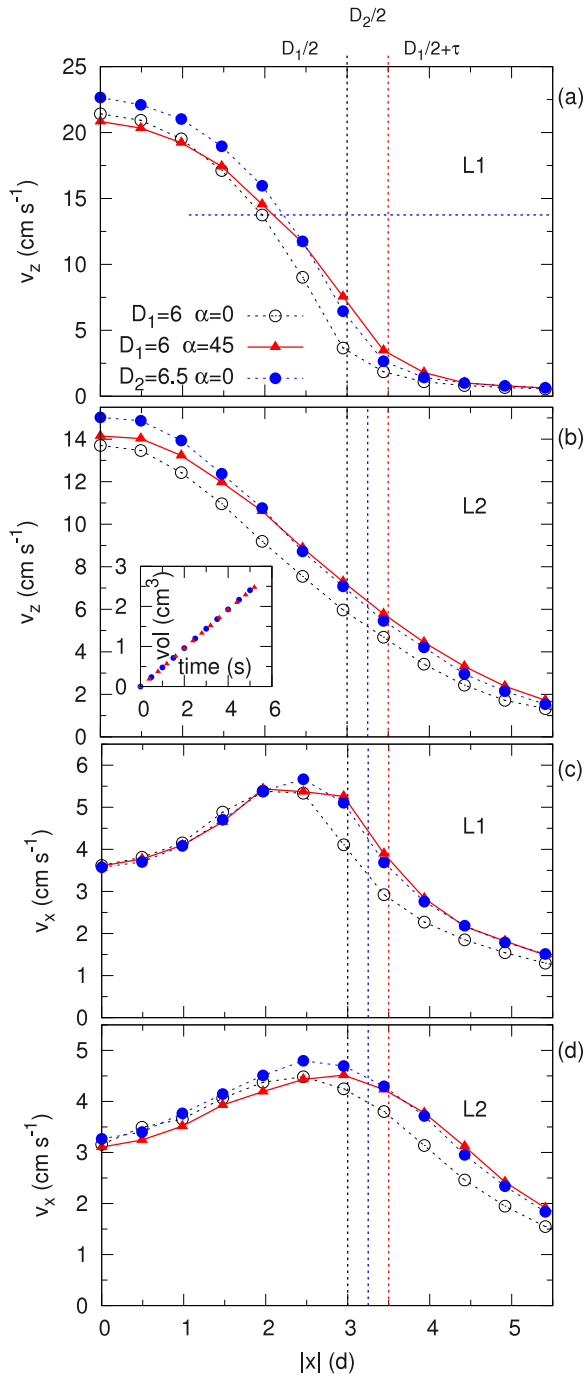

Fig. 8. (a) v_z as a function of the distance from the center of the container x at the bottom of the silo ($L1 : z = (0 - 2d)$) and (b) at a height $L2 : z = (2d - 4d)$ above the bottom. Two different openings with slant angle $\alpha = 0°$are represented in dashed lines, $D_1 = 6.0d$ (open black circles) and $D_2 = 6.5d$ (filled blue circles). Red triangles and continuum line represents the case with opening D_1 and $\alpha = 45°$. (c) and (d) are the same than (a) and (b) but for v_x. The inset in (b) highlights the equivalence in flow rate for systems $(6d, 45°)$ and $(6.5d, 0°)$.Vertical dashed lines mark the positions corresponding to the two outlet openings $x = D_1/2 = 3d$ and $x = D_2/2 = 3.25d$, and the inflection point of the bevel for D_1, $x = D_1/2 + \tau$.

CRediT authorship contribution statement

Paula A. Gago: Conceptualization, Conducted the numerical simulations and produced the numerical results, Writing – original draft. **Marcos A. Madrid:** Conceptualization, Writing – original draft. **Stefan Boettcher:** Data discussion, Draft revision. **Raphael Blumenfeld:** Data discussion, Draft revision. **Peter King:** Data discussion, Draft revision.

Declaration of competing interest

The authors declare that they have no known competing financial interests or personal relationships that could have appeared to influence the work reported in this paper.

Data availability

Data will be made available on request.

Acknowledgements

We thank Universiti Teknologi Brunei for their support of this work as a component of their sand screen retention project. Simulations were performed at the Imperial College Research Computing Service (see DOI: 10.14469/hpc/2232). MAM would like to thank the financial support from ANPCyT (Argentina) through Grant PICT 2020-SERIEA-02611 and UTN (Argentina) through Grant PID MAUTNLP0006542.

References

[1] C. Mankoc, A. Janda, R. Arevalo, J.M. Pastor, I. Zuriguel, A. Garcimartín, D. Maza, The flow rate of granular materials through an orifice, Granul. Matter 9 (2007) 407–414.
[2] A. Janda, I. Zuriguel, D. Maza, Flow rate of particles through apertures obtained from self-similar density and velocity profiles, Phys. Rev. Lett. 108 (2012) 248001.
[3] P.A. Gago, D.R. Parisi, L.A. Pugnaloni, Faster is slower effect in granular flows, Traffic Granul. Flow 11 (2013) 317–324.
[4] I. Zuriguel, D.R. Parisi, R.C. Hidalgo, C. Lozano, A. Janda, P.A. Gago, J.P. Peralta, L.M. Ferrer, L.A. Pugnaloni, E. Clément, D. Maza, Clogging transition of many-particle systems flowing through bottlenecks, Sci. Rep. 4 (2014) 1–8.
[5] M.A. Madrid, J.R. Darias, L.A. Pugnaloni, Forced flow of granular media: Breakdown of the beverloo scaling, Europhys. Lett. 123 (2018) 14004.
[6] J.R. Darias, M.A. Madrid, L.A. Pugnaloni, Differential equation for the flow rate of discharging silos based on energy balance, Phys. Rev. E 101 (2020) 052905.
[7] Florencia G. Escudero Acuña, Marcela C. Villagrán Olivares, Jesica G. Benito, Ana M. Vidales, Kinematics of the discharge of flat particles from model silos, Granul. Matter 24 (2022) 102.
[8] Ahmed Hafez, Qi Liu, Thomas Finkbeiner, Raed A. Alouhali, Timothy E. Moellendick, J. Carlos Santamarina, The effect of particle shape on discharge and clogging, Sci. Rep. 11 (2021) 3309.
[9] Fernando Alonso-Marroquin, Peter Mora, Beverloo law for hopper flow derived from self-similar profiles, Granul. Matter 23 (2020) 7.
[10] M. Benyamine, M. Djermane, B. Dalloz-Dubrujeaud, P. Aussillous, Discharge flow of a bidisperse granular media from a silo, Phys. Rev. E 90 (2014) 032201.
[11] Roberto. Arévalo, Collisional regime during the discharge of a two-dimensional silo, Phys. Rev. E 105 (2022) 044901.
[12] F.G.R. Magalhães, A.P.F. Atman, J.G. Moreira, H.J. Herrmann, Analysis of the velocity field of granular hopper flow, Granul. Matter 18 (2016) 33.
[13] Wim A. Beverloo, Hendrik Antonie Leniger, J. Van de Velde, The flow of granular solids through orifices, Chem. Eng. Sci. 15 (1961) 260–269.
[14] D. Méndez, R.C. Hidalgo, D. Maza, The role of the hopper angle in silos: experimental and cfd analysis, Granul. Matter 23 (34) (2021) 1–13.
[15] Xuezhi Zhang, Sheng Zhang, Guanghui Yang, Ping Lin, Yuan Tian, Jiang-Feng Wan, Lei Yang, Investigation of flow rate in a quasi-2d hopper with two symmetric outlets, Phys. Lett. A 380 (2016) 1301–1305.
[16] Sara M. Rubio-Largo, A. Janda, D. Maza, I. Zuriguel, R.C. Hidalgo, Disentangling the free-fall arch paradox in silo discharge, Phys. Rev. Lett. 114 (2015) 238002.
[17] R.M. Nedderman, Statics and kinematics of granular materials, 352, 1992.
[18] R.L. Brown, J.C. Richards, Principles of powder mechanics: essays on the packing and flow of powders and bulk solids, 10, 2016.
[19] L. Kondic, Simulations of two dimensional hopper flow, Granul. Matter 16 (2014) 235–242.
[20] L.A. Pugnaloni E. Goldberg, C.M. Carlevaro, Flow rate of polygonal grains through a bottleneck: Interplay between shape and size, Papers in physics 7 (2015).
[21] N. Govender, D.N. Wilke, Chuan-Yu Wu, J. Khinast, P. Pizette, Wenjie Xu, Hopper flow of irregularly shaped particles (non-convex polyhedra): Gpu-based dem simulation and experimental validation, Chem. Eng. Sci. 188 (2018) 34–51.
[22] Nan Gui, Xingtuan Yang, Jiyuan Tu, Shengyao Jiang, Flow fields and packing states in the discharge flow of noncircular particles—A siphpm simulation, Particuology 35 (2017) 10–21.

[23] L. Staron, P.-Y. Lagrée, S. Popinet, The granular silo as a continuum plastic flow: The hour-glass vs the clepsydra, Phys. Fluids 24 (2012) 103301.
[24] Jiangfeng Wan, Fugang Wang, Guanghui Yang, Sheng Zhang, Mengke Wang, Ping Lin, Lei Yang, The influence of orifice shape on the flow rate: A dem and experimental research in 3d hopper granular flows, Powder Technol. 335 (2018) 147–155.
[25] R.L. Brown, Minimum energy theorem for flow of dry granules through apertures, Nature 191 (1961) 458–461.
[26] C. Kloss, C. Goniva, A. Hager, S. Amberger, S. Pirker, Models, algorithms and validation for opensource dem and cfd–dem, Prog. Comput. Fluid Dyn. Int. J. 12 (2012) 140–152.
[27] I. Zuriguel, A. Garcimartín, D. Maza, L.A. Pugnaloni, J.M. Pastor, Jamming during the discharge of granular matter from a silo, Phys. Rev. E 71 (2005) 051303.